GROUND STATE OF BOSE-EINSTEIN CONDENSATES WITH INHOMOGENEOUS SCATTERING LENGTHS

A.I. NICOLIN[1,*], A. BALAŽ[2], J.B. SUDHARSAN[3], R. RADHA[3]

[1]Horia Hulubei National Institute for Physics and Nuclear Engineering, Reactorului 30, Magurele, Romania

[2]Scientific Computing Laboratory, Institute of Physics Belgrade, University of Belgrade, Pregrevica 118, 11080 Belgrade, Serbia

[3]Centre for Nonlinear Science, Post-Graduate and Research Department of Physics, Government College for Women (Autonomous), Kumbakonam – 612001, India

E-mail[*]: alexandru.nicolin@nipne.ro (corresponding author)

Received October 1, 2013

We show through detailed numerical investigations and supporting variational results that the ground state of a cigar-shaped Bose-Einstein condensate with a Gaussian-shaped radially inhomogeneous scattering length has a density profile akin to that of a coaxial cable. Monitoring the transition from homogeneous to inhomogeneous scattering lengths, we show numerically the formation of a local minimum in the density profile of the ground state positioned where the scattering length reaches its maximum.

1. INTRODUCTION

Over the past two decades, the ground state properties of Bose-Einstein condensates (BECs) have been subject to recurrent theoretical and computational investigations motivated by a long series of experiments with atomic species as different as rubidium and dysprosium (see Ref. [1] for a textbook introduction). The $T = 0$ properties of BECs are governed by a nonlinear Schrödinger equation with cubic nonlinearity, the so-called Gross-Pitaevskii equation (GPE), for whose solving, we now have accurate numerical algorithms (see Refs. [2–4]) and detailed analytical results (see Ref. [5] and references therein). The early works on the subject reported results obtained by variational means for the density profiles of three-dimensional condensates with repulsive and attractive interactions confined by parabolic magnetic fields. These initial theoretical investigations were focused on the bulk properties of the condensates and relied on Gaussian functions to describe the wave function of the condensate (see, for instance, the classical treatment in Ref. [6]). Similar variational treatments tailored around Gaussian functions have been used in nonlinear optics to describe the propagation of light pulses in nonlinear media [7]. More detailed studies on the ground state properties of high-density condensates have shown that the Gaussian functions are inaccurate in this regime and that the Thomas-Fermi approximation is better suited (see the discussion in chapter 6 of Ref. [1]). Moreover, for the surface structure of condensates, it was shown that one has to employ more complex functions (such as those proposed in Ref. [8] or the q-Gaussians proposed in Ref. [5]) which describe both the bulk properties of the condensate and its surface. Finally, we notice that the analytic information concerning the ground-state of one-dimensional condensates was used to craft effectively one- and two-dimensional equations for the dynamics of cigar-shaped and pancake-shaped three-dimensional condensates (see Refs. [9–11] for the low-density regime and Refs. [12–15] for the high-density regime). We also observe the existence of the analytically exact solitonic stationary states which are known for a wide variety of experimental setups [16–18].

The simple picture depicted above changes for condensates consisting of two (or more) atomic species, as their ground state configurations can be either miscible or non-miscible. In the miscible case, the wave functions overlap and the previous variational calculation can be easily extended due to the localized nature of the ground state. Non-miscible configurations, however, are qualitatively different, as the ground state configurations exhibit symbiotic structures which can not be described in terms of simple localized states and made-to-measure variational models have to be used (see Ref. [19] for an example).

2. THE GROSS-PITAEVSKII EQUATION

The ground state properties and the dynamics of a three-dimensional BEC are accurately described close to $T=0$ by the time-independent

$$-\frac{\hbar^2}{2m}\nabla^2\psi(\mathbf{r})+V(\mathbf{r})\psi(\mathbf{r})+g(\mathbf{r})\left|\psi(\mathbf{r})\right|^2\psi(\mathbf{r})=0 \tag{1}$$

GPE, while the time-dependent GPE

$$i\hbar\frac{\partial\psi(\mathbf{r},t)}{\partial t}=-\frac{\hbar^2}{2m}\nabla^2\psi(\mathbf{r},t)+V(\mathbf{r})\psi(\mathbf{r},t)+g(\mathbf{r},t)\left|\psi(\mathbf{r},t)\right|^2\psi(\mathbf{r},t) \tag{2}$$

describes the dynamics, where

$$V(\mathbf{r})=\frac{m}{2}\left(\Omega_\rho\rho^2+\Omega_z z^2\right)$$

represents the external trapping potential and $g=4\pi\hbar^2 a_s/m$ describes the strength of the nonlinear interaction. As the scattering length a_s can be modulated in time and space through Feshbach resonances (either magnetically [20, 21] or optically[22]), one has excellent experimental control over the nonlinear term. This notable level of experimental control inspired many theoretical works devoted to investigating the dynamics of condensates subjected to temporal and/or spatial modulation of the nonlinear interaction. In particular, the application of such a Feshbach resonance management technique [23] in the temporal domain can be used to stabilize attractive higher-dimensional condensates against collapse [24, 25], and also to create robust matter-wave breathers (in the effectively 1D setting) [23, 26].

Equations (1) and (2) are akin to the Ginzburg-Landau equations used in the early fifties to model superconductivity and very similar nonlinear equations have been used for the weakly nonlinear dynamics of a wave train propagating at the surface of a liquid (the so-called water-wave problem), the Langmuir oscillations (also referred to as Langmuir waves or electron plasma waves) that arise in non-magnetized or weakly magnetized plasmas, the Alfvén waves that propagate along an ambient magnetic field in a quasi-neutral plasma, and many other problems (see Ref. [27] for a detailed discussion).

In this paper, we consider the Gaussian-shaped spatially inhomogeneous interaction

$$g(\mathbf{r}) = \frac{4\pi\hbar^2 a_s}{m} \exp\left(-\frac{\rho^2}{2b^2}\right) \tag{3}$$

$$= g_0 \exp\left(-\frac{\rho^2}{2b^2}\right), \tag{4}$$

characterized by a parameter b. Condensates subjected to such an interaction are usually refered to as collisionally inhomogeneous condensates [28] and they are known to support a variety of new nonlinear phenomena. These include the adiabatic compression of matter-waves [28, 29], Bloch oscillations of matter-wave solitons [28], atomic soliton emission and atom lasers [30], dynamical trapping of matter-wave solitons [31, 32], enhancement of transmissivity of matter-waves through barriers [32, 33], the formation of stable condensates exhibiting both attractive and repulsive interatomic interactions [34], the delocalization transition in optical lattices [35], spontaneous symmetry breaking in a nonlinear double-well pseudopotential [36], the competition between incommensurable linear and nonlinear lattices [37] (for a review on the topic of nonlinear lattices see Ref. [38]), the generation of dark and bright solitons [39] and vortex rings [40], and many others.

We solve the time-independent GPE for a system with $\Omega_\rho = 160 \cdot 2\pi$ Hz, $\Omega_z = 7 \cdot 2\pi$ Hz, $N = 2.5 \cdot 10^5$ atoms of ^{87}Rb using the parallelized version of the GPE solvers introduced in Ref. [4]. On the analytical side, one can simplify the GPE to a system of algebraic equations by variational means. To this end, one starts from the associated Lagrangian density

$$\mathcal{L}(\mathbf{r}) = \frac{\hbar^2}{2m} |\nabla\psi(\mathbf{r})|^2 + V(\mathbf{r})\,|\psi(\mathbf{r})|^2 + \frac{g(\mathbf{r})N}{2} |\psi(\mathbf{r})|^4 \tag{5}$$

and the trial wave function

$$\psi(\mathbf{r}) = A\left(1+\gamma\rho^2\right) \exp\left(-\frac{\rho^2}{2w_\rho^2}\right) \exp\left(-\frac{z^2}{2w_z^2}\right), \tag{6}$$

where

$$A = \left(\pi^{3/2} w_\rho^2 w_z + 2\pi^{3/2} w_\rho^4 w_z \gamma + 2\pi^{3/2} w_\rho^6 w_z \gamma^2\right)^{-1/2}, \tag{7}$$

such that the wave function is normalized to unity and γ is a large parameter. The next step is to minimize the ensuing Lagrangian with respect to the variational parameters w_ρ, w_z and γ. Computing the Lagrangian is straightforward and one finds without difficulty that

$$\begin{aligned} L =& \int d\mathbf{r} \mathcal{L}(\mathbf{r}) \\ =& \frac{1}{4}\left(\frac{2^{3/2} b^2 g_0 N \left(s^4 + 8b^2 w_\rho^2 s^3 \gamma + 48 b^4 w_\rho^4 s^2 \gamma^2 + 192 b^6 w_\rho^6 s \gamma^3 + 384 b^8 w_\rho^8 \gamma^4\right)}{\pi^{3/2} s^5 w_z \left(w_\rho + 2 w_\rho^3 \gamma + 2 w_\rho^5 \gamma^2\right)^2}\right. \\ & m\left(\frac{2 w_\rho^2 \Omega_\rho^2 \left(1 + 4 w_\rho^2 \gamma + 6 w_\rho^4 \gamma^2\right)}{1 + 2 w_\rho^2 \gamma \left(1 + w_\rho^2 \gamma\right)} + w_z^2 \Omega_z^2\right) \\ & \left. + \frac{\hbar^2 \left(w_\rho^2 + 2 w_z^2 + 2 w_\rho^6 \gamma^2 + 2 w_\rho^4 \gamma \left(1 + 2 w_z^2 \gamma\right)\right)}{m w_\rho^2 w_z^2 \left(1 + 2 w_\rho^2 \gamma \left(1 + w_\rho^2 \gamma\right)\right)}\right), \end{aligned}$$

where $s = 4b^2 + w_\rho^2$.

The minimization yields the following three algebraic equations

$$\frac{\partial L}{\partial w_\rho} = 0, \tag{8}$$

$$\frac{\partial L}{\partial w_z} = 0, \tag{9}$$

$$\frac{\partial L}{\partial \gamma} = 0. \tag{10}$$

which are not amenable to analytic manipulations. However, as γ is large, one can solve equation (10) up to terms $\mathcal{O}\left(\gamma^{-4}\right)$ and smaller which yields

$$\gamma = \frac{24\sqrt{2} b^6 g_0 m N w_\rho^4 + 2\pi^{3/2} s^5 w_z \hbar^2}{m w_\rho^4 \left(\pi^{3/2} w_\rho^2 w_z \hbar^2 s^5 + m \pi^{3/2} w_\rho^2 w_z \Omega_\rho^2 s^5 - 48\sqrt{2} b^8 g_0 N\right)}. \tag{11}$$

The equations for w_ρ and w_z can then be simplified to

$$\begin{aligned} 4m\pi^{3/2} w_\rho^4 \left(4b^2 + w_\rho^2\right)^6 w_z \Omega_\rho^2 \hbar^2 - 12\sqrt{2} b^6 g_0 N \left(8m^2 w_\rho^6 b^4 \Omega_\rho^2\right.& \\ \left. -3m^2 w_\rho^6 w_z^4 \Omega_\rho^2 + \left(4b^2 + w_\rho^2\right)\left(8b^4 + 16 b^2 w_\rho^2 + w_\rho^4\right)\hbar^2\right) &= 0, \quad (12) \\ -\frac{42\sqrt{2} g_0 N w_z \left(b^8 + 2b^{10}\gamma\right)}{\pi^{3/2} w_\rho^2 \left(4b^2 + w_\rho^2\right)^5 \gamma} + m w_z^4 \Omega_z^2 - \frac{\hbar^2}{m} &= 0, \quad (13) \end{aligned}$$

where we have neglected terms $\mathcal{O}\left(\gamma^{-2}\right)$ and smaller. As we will see, these algebraic equations describe accurately the ground state of the condensate independent of the value of the parameter b and represent the main analytical result of our paper.

3. RESULTS AND CONCLUSION

We have monitored the density profile of a condensate with $N = 2.5 \cdot 10^5$ atoms of ^{87}Rb loaded in a magnetic trap with frequencies $\Omega_\rho = 160 \cdot 2\pi$ Hz and $\Omega_z = 7 \cdot 2\pi$ Hz. We have first determined the ground state of the condensate for a spatially homogeneous scattering length, corresponding to a limit $b \to \infty$, and set the radial width of the longitudinally-integrated density profile of the condensate, hereafter referred to as b_0, as our reference value for b. For the system under investigation our numerical simulations show that this value is $b_0 = 1.859$ μm.

For values of b larger than b_0, the ground state of the condensate is very similar to that of a condensate with spatially homogeneous two-body interactions. As expected, the Gaussian approximation fails to describe quantitatively the density profile of the condensate (which is, in fact, in the Thomas-Fermi regime), but it gives nevertheless a clear overall picture regarding the peak density of the condensate and its longitudinal extent. There is, in fact, a long series of investigations which use the Gaussian approximation to describe high-density (or, equivalently, strongly interacting) condensates and they all show that despite the apparent quantitative differences, the approximation describes accurately the energy of the condensate and its dynamical properties [6, 9, 41, 42, 44, 43, 45, 46].

In Fig. 1, we show the radial density profile of the condensate for b equal to b_0, $2b_0$, $4b_0$ and $b \to \infty$ using both the full GPE numerics and the simplified variational equations introduced in the previous section. We notice that the variational results always exhibit a small cusp in a vicinity of $\rho = 0$ which is due to hybrid nature of our trial wave function which combines a polynomial with a set of Gaussian functions. As the parameter b gets closer to b_0, one notices the formation of a small dip in the radial density profile which is positioned at $\rho = 0$. The decreased density at $\rho = 0$ corresponds to the formation of a small local maximum in the scattering length and this effect increases in visibility as b gets smaller.

The formation of the density dip is depicted in Fig. 2 where we show the radial density profile for b equal to $b_0/2$ and $b_0/4$. We observe that in this case, the numerical results are in excellent agreement with the variational investigations as the maximal value of the interaction along the $\rho = 0$ line makes the condensate an effectively low-density one (or, equivalently, weakly-interacting) and the Gaussian ansatz describes very accurately the cut-off of the wave function at large values of ρ. We also notice that for $b = b_0/2$, the condensate density in the center of the trap decreases by a factor of 2, while for $b = b_0/4$, the density decreases by an order of magnitude and the condensate looks almost depleted of atoms at $(\rho, z) = (0, 0)$. For

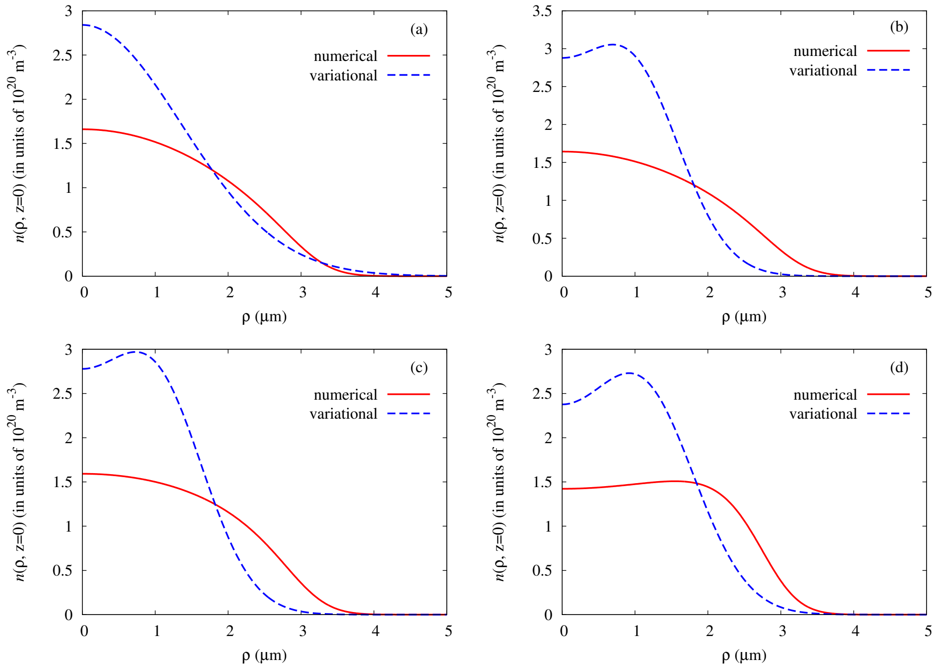

Figure 1 – Radial density profile of the condensate for $z = 0$ and: (a) $b \to \infty$, (b) $b = 4b_0$, (c) $b = 2b_0$, (d) $b = b_0$. The full red line shows the numerical results obtained from the GPE while the dashed blue line corresponds to the numerical solution of the variational equations. Notice that the variational results always exhibit a small cusp in a vicinity of $\rho = 0$, while the full numerical results show that it only appears for b close to b_0, panel (d).

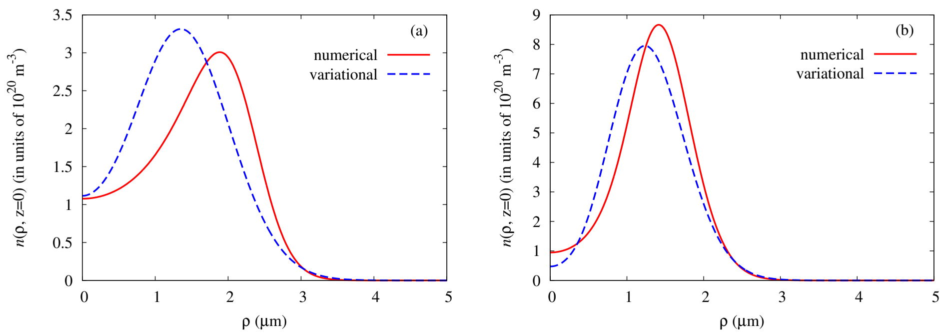

Figure 2 – Radial density profile of the condensate for $z = 0$ and: (a) $b = b_0/2$, (b) $b = b_0/4$. The full red line shows the numerical results obtained from the GPE while the dashed blue line corresponds to the numerical solution of the variational equations. Notice that for $b = b_0/4$, the density in the center of the condensate, *i.e.*, $(\rho, z) = (0, 0)$, is smaller by an order of magnitude than its peak value.

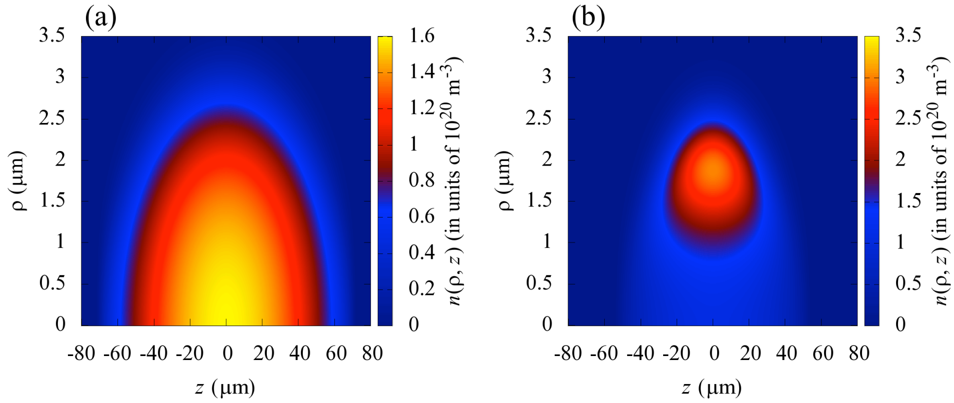

Figure 3 – Density profile of the condensate for: (a) $b = 2b_0$, (b) $b = b_0/2$. The profile for $b = 2b_0$ corresponds to the longitudinal density profile depicted in Fig. 1(c), while the profile for $b = b_0/2$ corresponds to the longitudinal density profile depicted in Fig. 2(a).

such small values of b, our ansatz effectively reduces to

$$\psi(\mathbf{r}) = \frac{\rho^2}{\sqrt{2\pi^{3/2}w_\rho^6 w_z}} \exp\left(-\frac{\rho^2}{2w_\rho^2}\right) \exp\left(-\frac{z^2}{2w_z^2}\right), \tag{14}$$

and the corresponding variational equations for the radial and longitudinal width of the condensate are given by

$$4m\pi^{3/2}w_\rho^4\left(4b^2+w_\rho^2\right)^6 w_z\Omega_\rho^2\hbar^2 - 12\sqrt{2}b^6 g_0 N\left(8m^2w_\rho^6 b^4\Omega_\rho^2 - 3m^2w_\rho^6 w_z^4\Omega_\rho^2 + \left(4b^2+w_\rho^2\right)\left(8b^4+16b^2w_\rho^2+w_\rho^4\right)\hbar^2\right) = 0, \tag{15}$$

$$-96\sqrt{2}b^{10}g_0 mNw_z + \pi^{3/2}w_\rho^2\left(4b^2+w_\rho^2\right)^5\left(m^2w_z^4\Omega_z^2-\hbar^2\right) = 0. \tag{16}$$

Finally, we depict in Fig. 3, the $\rho - z$ density profile of the condensate for b equal to $2b_0$ and $b_0/2$. The results in Fig. 3(a) show that the wave function of the condensate has a clear maximum at $\rho = 0$ and that it fades out for increasing values of ρ. This behavior is typical for condensates with homogeneous scattering length and is in clear violation of numerical results in Fig. 3(b), where one observes the wave function slowly increasing as ρ increases from 0 to 1.9 μm and then abruptly fading out for larger vales of ρ.

In conclusion, we have performed a series of detailed numerical investigations for the ground state of a cigar-shaped Bose-Einstein condensate subject to a Gaussian-shaped radially inhomogeneous scattering length and have shown that its density profile is similar to that of a coaxial cable. The numerical results are strengthened by a variational treatment which supports our numerical results and allows for a simple description of the ground state using only two algebraic equations. We plan to extend the current results to binary mixtures and study the emergence of density waves in condensates with inhomogeneous scattering lengths complementing the very recent analytical results from Ref. [47] with detailed numerical simulations. Also on the side of future investigations, we plan to study the dynamical stability of density waves with respect to thermal fluctuations. As the condensate particle loss is substantially higher after a parametric drive sets in, we expect that the interaction of the condensate with the non-condensed cloud can impact strongly the dynamics of the condensate for long time scales. To this end, we plan to graft self-consistently onto the Gross-Pitaevskii equation a Boltzmann transport equation which describes the thermal cloud in which the condensate is immersed.

Acknowledgements. For this work AIN was supported by a grant of the Romanian Ministry of Education, CNCS-UEFISCDI, project number PN-II-RU-PD-2012-3-0154. AB was supported in part by the Ministry of Education, Science, and Technological Development of the Republic of Serbia under Projects No. ON171017 and NAI-DBEC, by DAAD - German Academic and Exchange Service under Project NAI-DBEC, and by the European Commission under EU FP7 Projects PRACE-2IP, PRACE-3IP, HP-SEE, and EGI-InSPIRE. JBS wishes to acknowledge financial assistance from Department of Science and Technology (Ref. No. SR/S2/HEP-26/2012). The work of RR forms a part of University Grants Commission (Ref. No. UGC-40-420/2011 (SR)), Department of Atomic Energy - National Board of Higher Mathematics (Ref. No. DAE-NBHM-2/ 48(1)2010/NBHM-RD II/4524) and Department of Science and Technology (Ref. No. SR/S2/HEP-26/2012), Government of India sponsored projects.

REFERENCES

1. C.J. Pethick and H. Smith, *Bose-Einstein condensation in dilute gases* (Cambridge University Press, Cambridge, 2008).
2. S.K. Adhikari and P. Muruganandam, J. Phys. B: At. Mol. Opt. Phys. **35**, 2831 (2002).
3. P. Muruganandam and S.K. Adhikari, Comput. Phys. Commun. **180**, 1888 (2009).
4. D. Vudragović, I. Vidanović, A. Balaž, P. Muruganandam, and S. K. Adhikari, Comput. Phys. Commun. **183**, 2021 (2012).
5. A.I. Nicolin and R. Carretero-González, Physica A **387**, 6032 (2008).
6. G. Baym and C.J. Pethick, Phys. Rev. Lett. **76**, 6 (1996).
7. The Gaussian variational model and part of the ensuing applications of the variational equations to nonlinear processes such as parametric resonances and collision of solitons stem from nonlinear optics, where an equation that is mathematically identical to the GPE was used to describe the propagation of light pulses. To fathom the original calculations one can look into: E. Caglioti, S. Trillo, S. Wabnitz, B. Crosignani, and P. Di Porto, J. Opt. Soc. Amer. B **7**, 374 (1990); M. Desaix, D. Anderson, and M. Lisak, J. Opt. Soc. Amer. B **8**, 2082 (1991); B. Crosignani, P. Di Porto, and S. Piazzolla, Pure Appl. Opt. **1**, 7 (1992).
8. E. Lundh, C.J. Pethick, and H. Smith, Phys. Rev. A **55**, 2126 (1997).
9. L. Salasnich, A. Parola, and L. Reatto, Phys. Rev. A **65**, 043614 (2002).
10. L. Salasnich, Laser Phys. **12**, 198 (2002).

11. L. Salasnich, J. Phys. A: Math. Theor. **42**, 335205 (2009).
12. A. Muñoz Mateo, V. Delgado, Phys. Rev. A **77**, 013607 (2008).
13. A. Muñoz Mateo, V. Delgado, Ann. Phys. **324**, 709 (2009).
14. A.I. Nicolin, Rom. Rep. Phys. **61**, 641 (2009).
15. A.I. Nicolin and M.C. Raportaru, Physica A **389**, 4663 (2010).
16. B.A. Malomed, *Soliton Management in Periodic Systems* (Springer, New York, 2006).
17. D.J. Frantzeskakis, J. Phys. A: Math. Theor. **43**, 213001 (2010).
18. Y.V. Kartashov, B.A. Malomed, and L. Torner, Rev. Mod. Phys. **83**, 247 (2011).
19. A. Balaž and A.I. Nicolin, Phys. Rev. A **85**, 023613 (2012).
20. T. Kohler, K. Goral, and P.S. Julienne, Rev. Mod. Phys. **78**, 1311 (2006).
21. S. Inouye, M.R. Andrews, J. Stenger, H.-J. Miesner, D.M. Stamper-Kurn, and W. Ketterle, Nature (London) **392**, 151 (1998);
    J. Stenger, S. Inouye, M.R. Andrews, H.-J. Miesner, D.M. Stamper-Kurn, and W. Ketterle, Phys. Rev. Lett. **82**, 2422 (1999);
    J.L. Roberts, N.R. Claussen, J.P. Burke, Jr., C.H. Greene, E.A. Cornell, and C.E. Wieman, ibid. **81**, 5109 (1998);
    S.L. Cornish, N.R. Claussen, J.L. Roberts, E.A. Cornell, and C.E. Wieman, ibid. **85**, 1795 (2000).
22. F.K. Fatemi, K.M. Jones, and P.D. Lett, Phys. Rev. Lett. **85**, 4462 (2000);
    M. Theis, G. Thalhammer, K. Winkler, M. Hellwig, G. Ruff, R. Grimm, and J.H. Denschlag, ibid. **93**, 123001 (2004).
23. P.G. Kevrekidis, G. Theocharis, D.J. Frantzeskakis, and B.A. Malomed, Phys. Rev. Lett. **90**, 230401 (2003).
24. I. Towers and B.A. Malomed, J. Opt. Soc. Am. **19**, 537 (2002); see for a related experimental realization M. Centurion, M.A. Porter, P.G. Kevrekidis, and D. Psaltis, Phys. Rev. Lett. **97**, 033903 (2006);
    M. Centurion, M.A. Porter, Y. Pu, P.G. Kevrekidis, D.J. Frantzeskakis, and D. Psaltis, ibid. **97**, 234101; Phys. Rev. A **75**, 042902 (2008).
25. F.Kh. Abdullaev, J.G. Caputo, R.A. Kraenkel, and B.A. Malomed, Phys. Rev. A **67**, 013605 (2003);
    H. Saito and M. Ueda, Phys. Rev. Lett. **90**, 040403 (2003);
    G.D. Montesinos, V.M. Perez-Garcia, and P.J. Torres, Physica D **191**, 193 (2004).
26. D.E. Pelinovsky, P.G. Kevrekidis, and D.J. Frantzeskakis, Phys. Rev. Lett. **91**, 240201 (2003);
    D.E. Pelinovsky, P.G. Kevrekidis, D.J. Frantzeskakis, and V. Zharnitsky, Phys. Rev. E **70**, 047604 (2004);
    Z.-X. Liang, Z.-D. Zhang, and W.-M. Liu, Phys. Rev. Lett. **94**, 050402 (2005);
    M. Matuszewski, E. Infeld, B.A. Malomed, and M. Trippenbach, ibid. **95**, 050403 (2005).
27. C. Sulem and P.-L. Sulem, *The nonlinear Schrödinger equation* (Springer, New York, 1999).
28. G. Theocharis, P. Schmelcher, P.G. Kevrekidis, and D.J. Frantzeskakis, Phys. Rev. A **72**, 033614 (2005).
29. F.Kh. Abdullaev and M. Salerno, J. Phys. B **36**, 2851 (2003).
30. M.I. Rodas-Verde, H. Michinel, and V.M. Perez-Garcia, Phys. Rev. Lett. **95**, 153903 (2005);
    A.V. Carpenter, H. Michinel, M.I. Rodas-Verde, and V.M. Perez-Garcia, Phys. Rev. A **74**, 013619 (2006).
31. H. Sakaguchi and B.A. Malomed, Phys. Rev. E **72**, 046610 (2005); Phys. Rev. A **81**, 013624 (2010).
32. G. Theocharis, P. Schmelcher, P.G. Kevrekidis, and D.J. Frantzeskakis, Phys. Rev. A **74**, 053614 (2006); see also P. Niarchou, G. Theocharis, P.G. Kevrekidis, P. Schmelcher, and D.J. Frantzeskakis, Phys. Rev. A **76**, 023615 (2007) for a study of soliton oscillations in such settings.

33. F.Kh. Abdullaev and J. Garnier, Phys. Rev. A **74**, 013604 (2006).
34. G. Dong, B. Hu, and W. Lu, Phys. Rev. A **74**, 063601 (2006).
35. Yu.V. Bludov, V.A. Brazhhyi, and V.V. Konotop, Phys. Rev. A **76**, 023603 (2007).
36. T. Mayteevarunyoo, B.A. Malomed, and G. Dong, Phys. Rev. A **78**, 053601 (2008).
37. H. Sakaguchi and B.A. Malomed, Phys. Rev. A **81**, 013624 (2010);
F.Kh. Abdullaev, A. Abdumalikov and R. Galimzyanov, Phys. Lett. A **367**, 149 (2007).
38. Y.V. Kartashov, B.A. Malomed, and L. Torner, Rev. Mod. Phys. **83**, 247 (2011).
39. C. Wang, P.G. Kevrekidis, T.P. Horikis, and D.J. Frantzeskakis, Phys. Lett. A **374**, 3863 (2010);
H.J. Shin, R. Radha, and V. Ramesh Kumar, Phys. Lett. A **375**, 2519 (2011).
40. F. Pinsker, N.G. Berloff, and V.M. Perez-Garcia, Phys. Rev. A **87**, 053624 (2013).
41. A.I. Nicolin, M.H. Jensen, and R. Carretero-González, Phys. Rev. E **75**, 036208 (2007).
42. A.I. Nicolin, M.H. Jensen, J.W. Thomsen, and R. Carretero-González, Physica D **237**, 2476 (2008).
43. I. Vidanović, A. Balaž, H. Al-Jibbouri, and A. Pelster, Phys. Rev. A **84**, 013618 (2011).
44. A.I. Nicolin and M.C. Raportaru, Proc. Rom. Acad. Ser. A **12**, 209 (2011);
M.C. Raportaru, Rom. Rep. Phys. **64**, 105 (2012);
A.I. Nicolin, Proc. Rom. Acad. Ser. A **14**, 35 (2013).
45. A.I. Nicolin, Physica A **39**1, 1062 (2012).
46. H. Al-Jibbouri, I. Vidanović, A. Balaž, and A. Pelster, J. Phys. B: At. Mol. Opt. Phys. **46**, 065303 (2013).
47. S. Balasubramanian, R. Ramaswamy, and A.I. Nicolin, Rom. Rep. Phys. **65**, 820 (2013).